Pergamon

Int. J. Heat Mass Transfer. Vol. 39, No. 1, pp. 211–214, 1996

0017-9310/96 $9.50+0.00

0017-9310(95)00108-5

TECHNICAL NOTES

Heat transfer to sliding bubbles on a tube under evaporating and non-evaporating conditions

S. D. HOUSTON and KEITH CORNWELL†

Department of Mechanical and Chemical Engineering, Heriot-Watt University, James Nasmyth Building, Riccarton, Edinburgh EH14 4AS, U.K.

(*Received* 11 *August* 1994 *and in final form* 16 *February* 1995)

1. INTRODUCTION

It has been shown that much of the heat transfer which occurs when boiling on the outside of tube bundles under the low heat flux conditions used industrially is due to bubbles which slide around the tubes rather than by nucleation at the surface. These bubbles create a thin layer of liquid on the surface underneath them as they flow, causing local high heat transfer rates.

In previous experimental work [1, 2] it was possible to isolate the influence of these sliding bubbles under evaporating and condensing conditions by measuring the heat transfer and temperature of a designated test-cylinder within a tube bank over a wide range of conditions but independently of the overall tube bank conditions. This not only established the important role of these sliding bubbles but also enabled the different heat transfer coefficients for evaporation and condensing under similar conditions to be found. The condensing values were typically about half the evaporating values and some theoretical corroboration of this difference was presented.

This note reports an important extension of this work to non-evaporating (air) bubbles under similar conditions in an attempt to unravel further the complex heat transfer mechanisms associated with the sliding bubbles.

2. EVAPORATING AND CONDENSING TESTS

These tests are reported elsewhere [1, 2] and are merely summarized here as necessary background information. The boiling cell arrangement is shown in Fig. 1 and the tests were run using R113 at 1 atm at a constant mass flux of 95.1 kg $m^{-2} s^{-1}$. The Perspex boiling cell contained 34 tubes in two in-line columns, 33 being stainless steel tubes of 19.05 mm diameter on a 25.4 mm pitch and the test-cylinder being of copper and arranged as shown in Fig. 2. The central portion in between the sides of the boiling cell is heated by the two cartridge heaters or cooled by water flow through the copper coils.

The heat flux was measured by the temperature gradient along the 19.05 mm diameter copper rod as indicated by the thermocouples (T). These thermocouples consisted of chromel–alumel wires in a 1 mm diameter stainless steel sheath and were calibrated to give temperature readings accurate to 0.05°C. The heat flow differed by no more than 5% each side of the cell and an average value was taken. The surface temperature of the rod at the centre-line between the cell walls was estimated to within 0.1°C by radial conduction using a thermocouple situated 1.5 mm below the surface. The overall accuracy of the determination of the absolute heat transfer coefficient is 8–10% owing to the heat losses, the slight longitudinal gradient along the wall of the copper rod between the centre-line and the cell walls and thermocouple position errors. However, we are primarily concerned

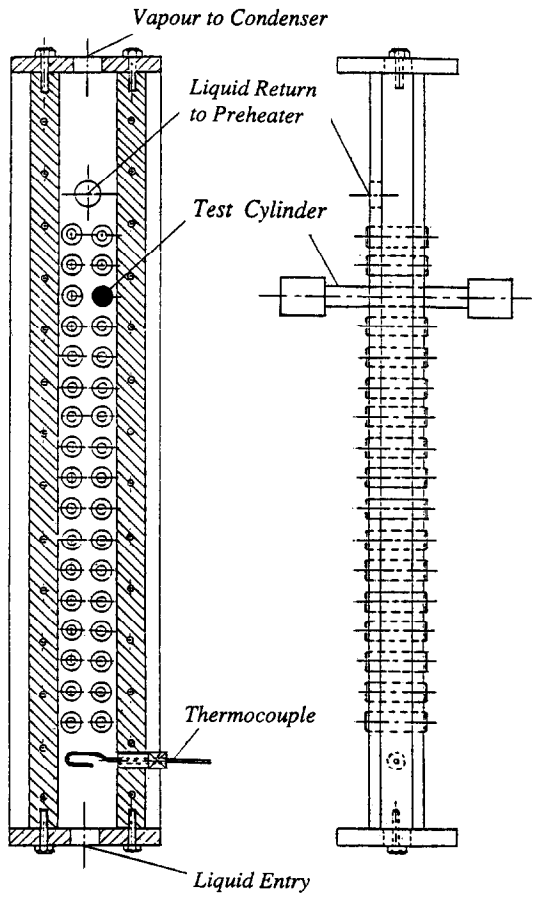

Fig. 1. Boiling cell used in evaporating and condensing tests (flow channel 25.4 × 50.8 mm).

†Author to whom all correspondence should be addressed.

NOMENCLATURE

q	heat flux at test cylinder [kW m^{-2}]	Greek symbols	
q_b	heat flux at other tubes in bundle [kW m^{-2}]	α	heat transfer coefficient
		ΔT	temperature difference [K]
		$\dot{v}$	air flow rate [l min^{-1}]

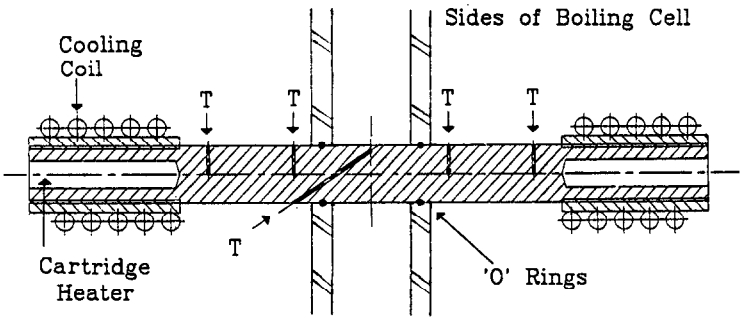

Fig. 2. Test-cylinder used for heating and cooling in the cell.

with relative effects between tests where the absolute errors are less important.

The tests were conducted by commencing at a high positive heat flux (causing evaporation at the tube) and reducing the heating in steps allowing about half an hour for stabilization. Following the step at zero current the process was continued by cooling the ends (causing condensation) until the maximum negative heat flux was reached. On most tests the process was subsequently reversed by progressing up the q–ΔT curve.

Typical results of these tests from ref. [2] are shown in Fig. 3 where the test-cylinder heat flux and wall-saturation temperature difference were measured at various bundle heat fluxes q_B at the other tubes. No hysteresis was observed at any bundle heat flux except that at zero when the test-cylinder was effectively operating under pool boiling conditions with no bubbles surrounding it from tubes below. Here hysteresis was noticed on the heating side, as normally found with pool-boiling.

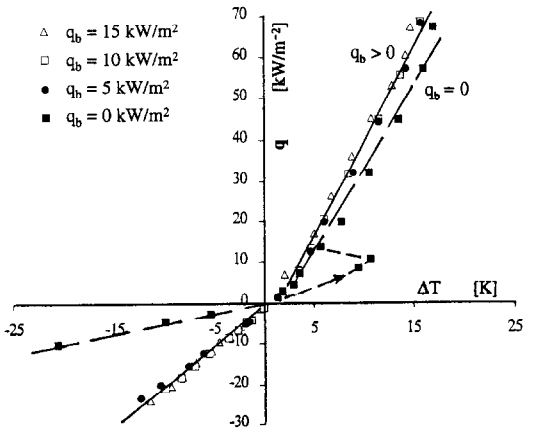

Fig. 3. Results for heating and cooling in the vapour flow at various bundle heat fluxes.

3. AIR FLOW TESTS

The purpose of these tests was to run the same test-cylinder under similar heating and cooling conditions, but in a bubbly air flow rather than a saturated vapour flow. It was anticipated that this would allow the possibility of separately identifying parts of the heat transfer mechanism due to thin layer evaporation or condensation and due to liquid convection with no two-phase heat transfer. For this purpose a new cell (shown in Fig. 4) was constructed with 25.4 mm channel width and 19.05 mm tube diameter as before, but with a single column of six tubes. The lowest tube at position 1 was an air-tube perforated with a large number of small holes to allow air to be injected into the system. The test-cylinder, again instrumented as shown in Fig. 2, was arranged in position 5 and the remaining four tubes were the same as those used in the previous rig.

The tests were run using R113 at 1 atm (boiling point, 47.6°C) and a constant mass flux of 95.1 kg m^{-2} s^{-1} as before, but at a nominal fluid inlet temperature of approximately 34°C (39°C for the no air flow case) rather than 47°C to avoid the possibility of evaporation at the surface of the tubes. The tests using the test-cylinder were conducted in the same way as described in Section 1 and the results are shown in Fig. 5. Air injection rates $\dot{v}$ were arranged to yield similar bubbly flow voidage around the test-cylinder, as experienced with the vapour flow under the evaporating conditions, by selecting the volmetric air flow rate to be approximately the same as the vapour flow rate.

4. DISCUSSION OF RESULTS

It would appear from the results shown in Fig. 5 that the heat transfer coefficient from the tube is fairly insensitive to the extent of bubbly flow as a factor of 5 difference in air flow injection rate yields very little difference in slope. This was also the case in Fig. 4 for vapour flow under evaporating and condensing conditions.

At a heating temperature difference of about 13°C the tube surface reaches the saturation temperature and sub-cooled boiling commences at some point above this threshold, thus accounting for the upward turn in the graph at high positive ΔT.

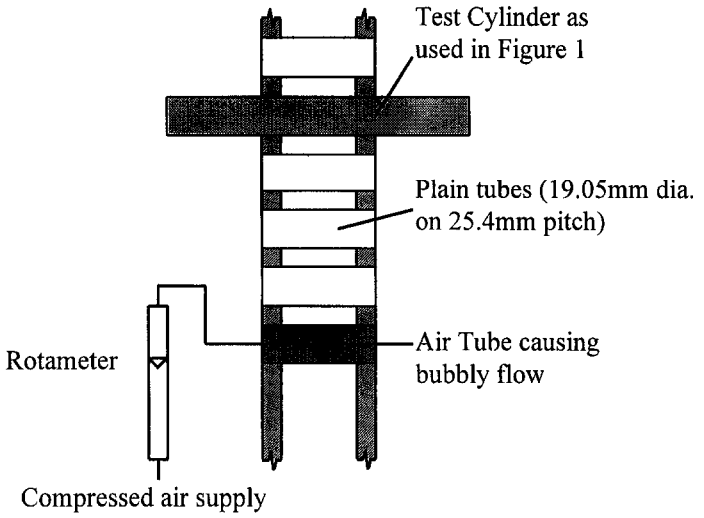

Fig. 4. Cell arrangement for air flow tests using the same test-cylinder.

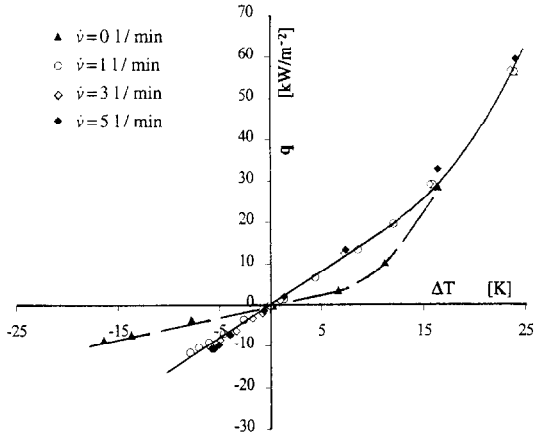

Fig. 5. Results for heating and cooling in the air flow at various injection rates.

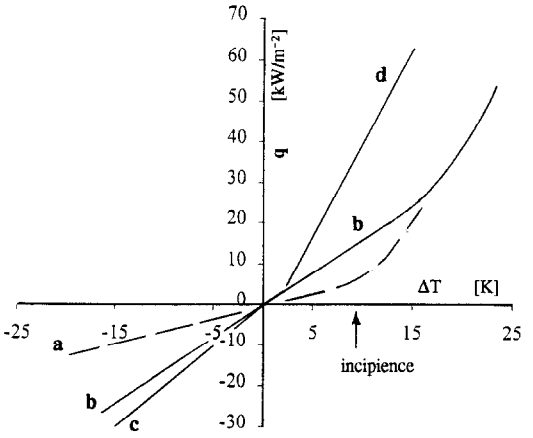

Fig. 6. Comparison of tests under vapour and air flow conditions.

The run with no air flow was obtained by commencing at a high heating heat flux well in the sub-cooled boiling region and lowering the heat flux in stages through zero into the cooling region (using the water cooling as before). Below the boiling range the constant slope represents liquid natural convection for the tube in this geometry and the results yield a similar slope to that for no vapour flow ($q_b = 0$) shown in Fig. 4.

For comparison purposes the mean curves in Figs. 3 and 5 are shown in Fig. 6 and the heat transfer coefficients (equal to the slopes if the small zero-point shift is ignored) at salient points are as shown in Table 1.

There are three significant conclusions which can be drawn from this additional work using air flow.

(1) Bubbly-flow turbulence is a prominent mechanism in the heat transfer.

(2) Condensation of the bubbles as they pass the tube does not add significantly to this heat transfer.

(3) Evaporation of the bubbles is a major factor but (at the low heat fluxes examined) is not significantly more than the bubbly-flow turbulence.

Theoretical analysis [2] of evaporation and condensation under a sliding bubble indicated that, for evaporation to account for the high α values, the liquid layer under the bubble must either be very thin (a few micrometres thick) or dry-out must occur. Condensation α values under the same conditions were shown to be lower.

This study indicates that heat transfer due to the turbulent convection mechanism caused by the translating bubble is at least as important as the mechanism in the layer under the bubble. Some corroboration of this is evident from recent work [3] on the influence of sliding bubbles on heat transfer from thin plates using thermochromic paints. Development

Table 1.

Point	Condition of flow	α value [kW m^{-2} K^{-1}]
a	No bubbles (liquid only)	0.5
b	Air bubbles	1.7
c	Condensing vapour bubbles	2.0
d	Evaporating vapour bubbles	4.7

of analysis accounting for the total heat transfer from the surface due to sliding bubbles must therefore include both mechanisms.

REFERENCES

1. K. Cornwell, The influence of bubbly flow on boiling from a tube in a bundle, *Int. J. Heat Mass Transfer* **33**, 2579–2584 (1990).
2. K. Cornwell, S. D. Houston and A. J. Addlesee, Sliding bubble heat transfer on a tube under heating and cooling conditions. In *Pool and External Flow Boiling* (Edited by V. K. Dhir and A. E. Bergles), pp. 49–53. New York ASME (1992).
3. Y. Yan and D. B. R. Kenning, Heat transfer near sliding vapour bubbles in boiling, *Tenth International Heat Transfer Conference, Brighton, U.K., Heat Transfer* 1994, Vol. 5, pp. 195–200 (1994).

Pergamon

Int. J. Heat Mass Transfer. Vol. 39, No. 1, pp. 214–218, 1996

0017-9310/96 $9.50+0.00

0017–9310(95)00074–7

Application of the diffuse approximation for solving fluid flow and heat transfer problems

H. SADAT and C. PRAX

Laboratoire d'Etudes Thermiques, URA CNRS 1403 ENSMA, Site du futuroscope, 86960 Futuroscope Cedex, France

(*Received* 7 *June* 1994 *and in final form* 15 *February* 1995)

1. INTRODUCTION

In the numerical simulation of fluid flow problems in regions with arbitrary shaped boundaries, finite-element methods (FEM) [1–3] and control-volume based finite-element methods [4–6] are generally used. For problems in which the position of large solution gradients is known *a priori*, such as those involving boundary layers, localized grid refinement can be used in these regions. There are several problems, however, where the position of steep gradients is not always known *a priori*. This is the case of compressible flows for example. Adaptive procedures for finite-element meshes are then necessary. Mesh generation and mesh enrichment are the most popular methods [7]. These techniques are time consuming and there is currently a great deal of research being done in this field [8].

The diffuse approximation method (DAM) is a new method for finding estimates of a scalar field φ and its derivatives [9, 10]. The starting point is to estimate the Taylor expansion of φ at a chosen point $M_i(x_i, y_i)$ by a weighted least squares method which uses only the values of φ at the nearest points $M_j(x_j, y_j)$. The main advantage of this method is that it only requires sets of discretization nodes and no geometric finite elements. These nodes could be generated by several techniques such as random shooting methods or octree-based methods. In any case it is much easier to generate nodal points than to build finite-element meshes. This method has been successfully used for steady-state diffusion problems [10, 11]. It has been shown that the DAM is much better than the FEM for the computation of gradients [9, 10]. Moreover it ensures uniform convergence of the successive derivate estimates when the sampling point density increases [10]. Application of the DAM to the post-treatment of electromagnetic field computations has been reported [12].

To date no attempt appears to have been made to apply the diffuse approximation in the field of computational fluid dynamics. Thus the main objective of this work is to demonstrate that this new method can be used to solve fluid flow and heat transfer problems with sufficient complexities that a fair test of the formulation can be made.

In the following sections, the formulation of the diffuse approximation is presented and applied to three example problems.

2. THE DIFFUSE APPROXIMATION

For a scalar field $\varphi(x, y)$ defined in a two-dimensional domain, let us pick a set of N points $M_i(x_i, y_i)$ in the vicinity of a chosen point $M(x, y)$. The diffuse approximation provides estimates of φ and its derivates at M from the nodal values φ_i. The basic idea is to estimate the Taylor expansion of φ at M by a weighted least squares method which uses only the values of φ at the nearest points M_i. By truncating the series at order k, one obtains the corresponding estimates of the derivatives at order k.

Therefore, as far as we are concerned by second-order partial differential equations, a second-order expansion is sufficient. Let us then estimate the second-order Taylor expansion of φ_i at M as:

$$\varphi_i = \sum_{j=0}^{5} P_{ij} \cdot \alpha_j \tag{1}$$

where

$$[P_{ij}] = [1, (x_i - x), (y_i - y), (x_i - x)^2, (x_i - x) \cdot (y_i - y), (y_i - y)^2]$$

and